

See discussions, stats, and author profiles for this publication at: <https://www.researchgate.net/publication/261372324>

# Morphology of synthetic DOPA–eumelanin deposited on glass and mica substrates: An Atomic Force Microscopy investigation

ARTICLE in MICRON · SEPTEMBER 2014

Impact Factor: 1.99 · DOI: 10.1016/j.micron.2014.03.016

READS

80

## 9 AUTHORS, INCLUDING:



**Giuseppe Perna**

Università degli studi di Foggia

90 PUBLICATIONS 800 CITATIONS

SEE PROFILE



**Maria Lasalvia**

Università degli studi di Foggia

38 PUBLICATIONS 193 CITATIONS

SEE PROFILE



**Gerardo Palazzo**

Università degli Studi di Bari Aldo Moro

154 PUBLICATIONS 2,024 CITATIONS

SEE PROFILE



**Vito Capozzi**

Università degli studi di Foggia

175 PUBLICATIONS 1,599 CITATIONS

SEE PROFILE



# Morphology of synthetic DOPA-eumelanin deposited on glass and mica substrates: An atomic force microscopy investigation



G. Perna<sup>a</sup>, M. Lasalvia<sup>a</sup>, P. D'Antonio<sup>a</sup>, A. Mallardi<sup>b</sup>, G. Palazzo<sup>c</sup>,  
D. Fiocco<sup>a</sup>, A. Gallone<sup>d</sup>, R. Cicero<sup>a</sup>, V. Capozzi<sup>a,\*</sup>

<sup>a</sup> Dipartimento di Medicina Clinica e Sperimentale, Università degli studi di Foggia, Viale Pinto, 71122 Foggia, Italy

<sup>b</sup> CNR-IPCF, Istituto per i Processi Chimico-Fisici, UOS di Bari, 70126 Bari, Italy

<sup>c</sup> CSGI and Dipartimento di Chimica, Università di Bari, Via Orabona 4, 70126 Bari, Italy

<sup>d</sup> Dipartimento di Scienze Mediche di Base, Neuroscienze ed Organi di Senso, Università degli Studi di Bari "Aldo Moro", Policlinico-Piazza Giulio Cesare, 70124 Bari, Italy

## ARTICLE INFO

### Article history:

Received 20 January 2014

Received in revised form 25 March 2014

Accepted 30 March 2014

Available online 6 April 2014

### Keywords:

Eumelanin

Optical microscopy

Atomic force microscopy

Dynamic light scattering

## ABSTRACT

Bright field microscopy and atomic force microscopy techniques are used to investigate morphological properties of synthetic eumelanin, obtained by oxidation of L-DOPA solution, deposited on glass and mica substrates. Deposits of eumelanin are characterized by aggregates with different shape and size. On a micrometric scale, filamentous as well as granular structures are present on glass and mica substrates, with a larger density on the former than on the latter. On a nanometric scale, filamentous aggregates, several microns long and about 100 nm wide and high, and granular aggregates, ~50 nm high and 100 nm wide, are found on both substrates, whereas point-like deposits less than 10 nm high and less than 50 nm wide are found on mica substrate. Dynamic light scattering measurements and atomic force microscopy images support the evidence that eumelanin presents only nanometric point-like aggregates in aqueous solution, whereas such nanoaggregates organize themselves according to granular and filamentous structures when deposition occurs, as a consequence of interactions with the substrate surface.

© 2014 Elsevier Ltd. All rights reserved.

## 1. Introduction

Eumelanin is a widespread natural pigment, which is produced in animal pigment cells inside specialized organelles (melanosomes) by tyrosinase-catalyzed oxidation of tyrosine and the subsequent oxidation of the intermediate 3,4-dihydroxy-L-phenylalanine (L-DOPA) to yield L-dopaquinone and dopachrome and, finally, 5,6-dihydroxyindole (DHI) and 5,6-dihydroxyindole-2-carboxylic acid (DHICA) and their oxidized forms, according to the Raper–Mason melanogenesis pathway (Mason, 1948). Different combinations of such structural units combine themselves to make up protomolecules of eumelanin (Meredith and Sarna, 2006), although a fundamental role in the melanogenesis process is played by proteinaceous components, to which eumelanin is firmly bound through covalent and ionic bonds (Zeise, 1995), so that its ultrastructural organization is deeply influenced by this association. Accordingly, melanins are usually heterogeneous and complex, and

attempts to characterize their structure have led to a large amount of data, sometimes apparently contradictory (Liu and Simon, 2003).

Such biopolymer has optical and electrical properties which are interesting for a possible integration in photovoltaic (Morresi et al., 2010) and electronic devices (Ambrico et al., 2010). The molecular structure of eumelanin, whose understanding is fundamental to explain its physical properties in view of device applications, has been widely investigated (Meredith et al., 2006; Gallas et al., 1999; Watt et al., 2009; Jastrzebska et al., 2010), with the aim to identify the size of eumelanin protomolecules. Such issue is still under discussion, although during the last decades several theoretical and experimental investigations have supported a structural model based on the aggregation of few stacked planar sheets of the above structural units to form eumelanin protomolecules (Watt et al., 2009; Stark et al., 2003). Many experimental investigations involved different types of natural eumelanins, which include the protein components. Some other studies were based on different types of synthetic eumelanin, i.e. chemically prepared without protein content. In particular, natural eumelanins are important to investigate the structure-related functions of the pigment in living organisms, whereas the synthetic ones are fundamental samples to investigate the basic structural organization and physical

\* Corresponding author. Tel.: +39 0881588053.

E-mail addresses: [vito.capozzi@unifg.it](mailto:vito.capozzi@unifg.it), [capozzi@ba.infn.it](mailto:capozzi@ba.infn.it) (V. Capozzi).

properties of the biopolymer as promising technological material.

The sizes of eumelanin components have been widely investigated by means of optical techniques, such as absorption and fluorescence spectroscopy. In fact, absorption spectra of eumelanin are characterized by a strong absorption in UV and visible range with absorbance values nearly monotonically decreasing from UV to NIR, whereas fluorescence spectra of eumelanin present broad emission bands (Meredith et al., 2006; Perna et al., 2009, 2011). Both such types of spectra have been explained as due to the overlapping contributions of different eumelanin protomolecules having nanometer size. Nonetheless, such optical techniques allow to investigate the size of eumelanin components in an indirect way, i.e. the protomolecules size is deduced according to physical models which explain the experimental spectra.

A proper and direct tool to visualize the structure of eumelanin biopolymer at nanometer level is the atomic force microscopy (AFM) technique, because it can provide three-dimensional topographical information. In fact, also AFM studies confirmed the results of optical measurements and have supported the structural model of eumelanin as consisting of stacked oligomeric nanoaggregates, both for natural (Clancy and Simon, 2001) and synthetic eumelanins (Jastrzebska et al., 2010). Usually, eumelanin extracted from *Sepia officinalis* and eumelanin prepared by oxidation of L-DOPA are used as a model for natural and synthetic samples, respectively. Aqueous solution of such eumelanin samples are deposited on a proper substrate and AFM measurements are carried out after water evaporation and drying of the eumelanin deposit. AFM images of eumelanin from *S. officinalis* have revealed the presence of aggregate particles with diameters ranging from 100 to 200 nm and filament structures with average height and width of several nanometers and tens of nanometer, respectively (Clancy and Simon, 2001).

The AFM images reported up to now for synthetic eumelanin (obtained by oxidation of L-DOPA) are characterized by grains of transverse size of about 200 nm and height of several tens nanometer size, which self-assemble in fibril-like structures (Jastrzebska et al., 2010). However, no structures of few nanometer size (nearly “point-like” structures) have been observed for synthetic eumelanin, differently from natural eumelanin.

In this work, we discuss AFM images of synthetic eumelanin prepared from L-DOPA and deposited on glass and mica substrates. Our data demonstrate the presence of filamentous, granular and point-like nanometric structures. Many point-like structures on mica substrate have few nanometer height. We deduce, supported by dynamic light scattering (DLS) measurements, that only point-like structures are present in solution: they assemble to form granular and filamentous aggregates after deposition on the substrate, as a result of interaction among themselves and with the substrate surface.

## 2. Materials and methods

Samples of synthetic eumelanin were prepared starting from aqueous solution of 5 mM commercial L-DOPA (Sigma–Aldrich) in 5 mM Na-phosphate buffer (pH 7.2). L-DOPA solutions were aerated and stirred at room temperature for approximately 72 h, till their color became dark-brown, due to spontaneous oxidation and polymerization (Bridelli, 1998; Kruk et al., 1999). The 7.2 value of pH has been chosen because it is close to the physiological pH value. In fact, higher pH values could break the eumelanin granules (low degree of polymerization of eumelanin would result), whereas lower pH values could promote aggregation among single eumelanin grains (Crippa et al., 1989).

The samples for AFM investigation were obtained by depositing a droplet of eumelanin solution (about 40  $\mu$ l) onto a microscopy glass coverslip (previously rinsed with purified water) and a freshly cleaved mica substrate. The droplet was left in air at room temperature until the liquid was completely evaporated and the sample was dried.

A Perception (Assing S.p.A., Italy) Atomic Force Microscope was used to record AFM images. The measurements were performed in air, working in the weak repulsive regime of contact mode. Gold coated  $\text{Si}_3\text{N}_4$  V-shaped cantilevers with a nominal spring constant of 0.1 N/m and Silicon tips with a nominal apical radius of 20 nm were used for the topographic AFM images. Constant force images were acquired with a scan rate of about 7 s/row, at a resolution of  $256 \times 256$  points. The images were processed by means of the Gwyddion software package (Nečas and Klapetek, 2012).

DLS measurements of eumelanin in deionized water were performed using a Zetasizer-NanoS from Malvern operating with a 4 mW He–Ne laser (633 nm wavelength) and a fixed detector angle of  $173^\circ$  with respect to laser beam. The time Autocorrelation Function (ACF) of scattered light intensity was the average of 12–16 consecutive runs, each one of 10 s. The fraction of the light intensity scattered by particles of different sizes has been recorded by a photomultiplier tube. Size distribution of eumelanin particles suspension was obtained by taking the inverse Laplace transform of the ACF, using the software implemented by the manufacturer.

## 3. Results and discussion

### 3.1. Optical microscopy

Fig. 1 shows bright field microscopy images for synthetic eumelanin dried on a glass (a) and a mica (b) substrate. The liquid evaporation allows the eumelanin to be deposited onto a substrate surface. In particular, eumelanin deposit stands mainly at the edge of the evaporating fluid (region labeled EE in Fig. 1a) for the sample deposited on the glass substrate, where it makes a quite dense deposit consisting of filamentous structures having length of several hundreds micrometers and width of several micrometers. The accumulation of eumelanin particles on the edge of the evaporating drop is caused by the fluid flow from the center of the droplet forward the edge. Indeed, when water evaporates, the drop flattens (especially when the drop is deposited on a hydrophilic substrate, as glass and mica) and such flattening motion pushes water and particles suspended in it toward the edge. When the liquid is fully evaporated, most of the suspended particles have reached the edge, where they are deposited (Junker et al., 2011). The central region of the eumelanin deposit (labeled C in Fig. 1a) on glass substrate consists of sparse granular structures, which are barely visible in Fig. 1a. The region labeled IE in Fig. 1a, between the EE and C regions, consists of both filamentous and granular structures, with the former having lower density and the latter having larger density than similar structures on the EE and C region, respectively. On the contrary, the morphology of eumelanin deposit on mica substrate in Fig. 1b consists mainly of an external edge (region labeled EE in Fig. 1b) made of filamentous structures whose characteristics are similar to those on the IE region of Fig. 1a and a central region with very few granular material (not shown). Fig. 1b lacks of a region characterized by a dense eumelanin deposit (similar to EE region of Fig. 1a).

Similar filamentous structures have been observed upon drying of L-DOPA eumelanin solution at pH 10 on glass slide (McQueenie et al., 2012). Formation of eumelanin structures on solid surface involves several steps. Initially, spreading and flattening of

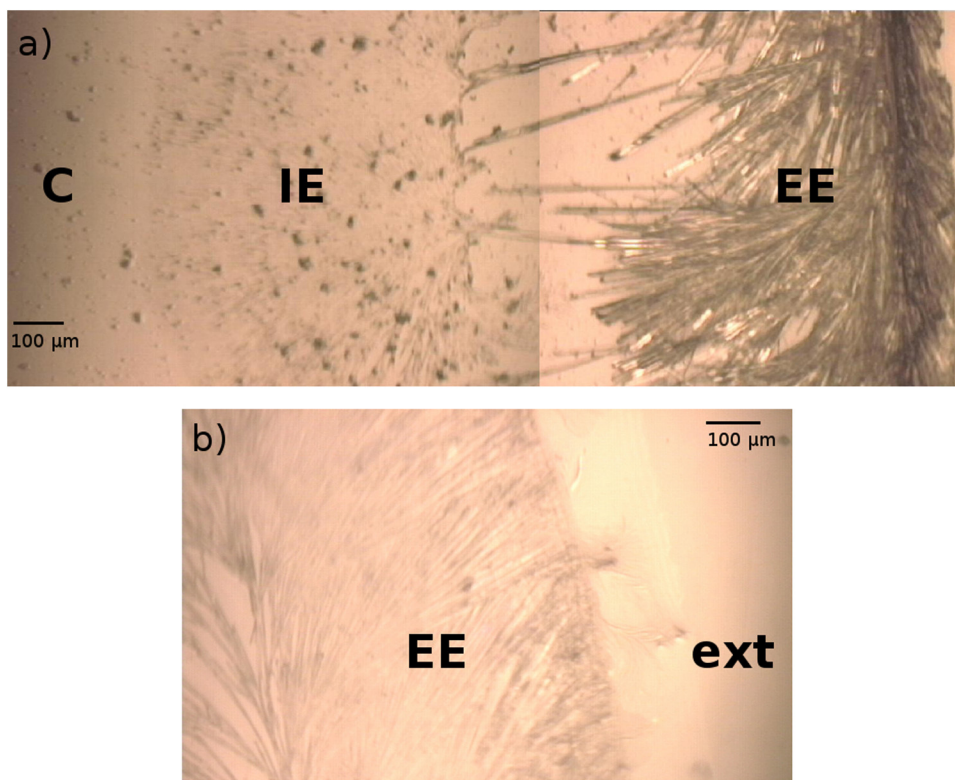


**Fig. 1.** Typical bright field microscopy images of synthetic L-DOPA eumelanin solution deposited and dried on a glass (a) and a mica (b) substrate. The label EE, IE and C stand for external edge, internal edge and central region, respectively, whereas ext refers to a region located externally with respect to eumelanin deposit (see text).

eumelanin drop on the substrate surface occurs, as previously discussed: such step is influenced by the nature of solid substrate. In particular, both glass and mica are hydrophilic materials, with mica even more hydrophilic than glass. So, a drop of aqueous solution spreads more easily on mica than on glass surface: consequently, the density of eumelanin structures deposited on glass is larger than that of structures deposited on mica. After evaporation of liquid component, eumelanin adsorbs from the solution onto the solid surface. According to the structure of eumelanin base units, their size, pH of solution and surface charge, the eumelanin components may either blend forming larger assemblies or remain intact during the adsorption process. Both glass and mica present a negatively charged surface (Erikson et al., 1997), so making quite easy the adsorption of eumelanin onto the substrate, although interactions between the eumelanin components and glass or mica substrate should be sufficiently weak to enable lateral movement of eumelanin components. Such interaction plays an important role in the process of formation of eumelanin structures by inducing reorganization of the eumelanin material cumulated on the substrate surface.

### 3.2. Atomic force microscopy

To better investigate the morphological structure of eumelanin deposit, we performed AFM measurements on the IE and C regions of glass substrate and the EE and C regions of mica substrate. The EE region of glass substrate has not been measured because of the large height of the deposited filamentous structures, which is beyond the dynamic properties of our AFM apparatus. On the other hand, the EE region is not properly interesting as the aim of our work is to investigate the morphology of the sub-micrometric eumelanin components. Fig. 2 shows typical height (a) and friction (b) images from the IE region of a synthetic eumelanin sample deposited on glass substrate. Such images are dominated by filamentous

eumelanin structures, almost parallel and partly overlapping each other. Linear profiles along the lines labeled 1 and 2 in Fig. 2a are shown in Fig. 2c. The size of such structures ranges from about 100 nm to about 150 nm of both height and width. In the bottom right angle of Fig. 1a, some eumelanin granules are clearly visible. The line profile along the line 3 in Fig. 2a, shown in Fig. 2c, shows that the size of such grains are about 30–50 nm height and 100 nm width (although the width might be overestimated because of tip-sample convolution effect). Therefore, as suggested in (Jastrzebska et al., 2010), we can suppose that such granules aggregate themselves, before water evaporation, to form the filamentous structures. Such hypothesis is in agreement with the structural model proposed for *S. officinalis* eumelanin starting from AFM measurements (Clancy and Simon, 2001). Such granules are also present in the C region of the eumelanin deposit on glass substrate, as can be deduced by a typical image of such region shown in Fig. 3a (height image) and Fig. 3b (friction image). The size of the grains in the C region is similar to that of granules in the IE region, as visible from line profiles 1 and 3 in Fig. 3c, but their density is lower in the former region, in agreement with the results discussed above for optical images. The line profile along the glass substrate, shown as line 2 in Fig. 3c, reveals the presence of structural features less than 10 nm size: these can be considered a background ripple related to experimental noise for glass substrate, although the contribution of smaller eumelanin grains (nearly “point-like” structures) cannot be excluded.

Fig. 4 shows AFM images of eumelanin deposit on mica substrate in the EE region. Filamentous as well as granular structures are clearly evident in both height (Fig. 4a) and friction (Fig. 4b) images. The width of filamentous structures ranges from about 100 nm to 150 nm and the height is about 100 nm (line profile 2 in Fig. 4c), whereas the granular features are about 100 nm wide and 50 nm high (line profile 3 in Fig. 4c). Similar grain size are found for several granular eumelanin structures in the central region of the mica



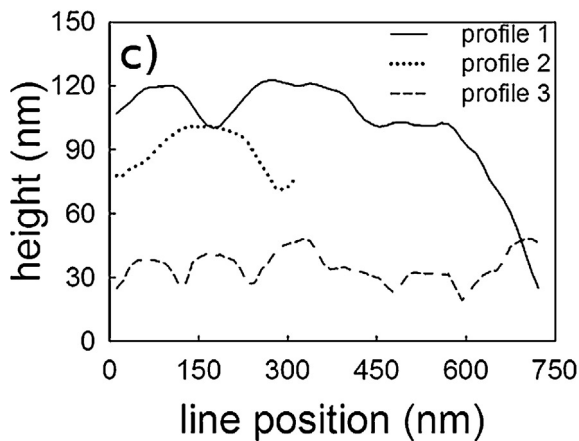
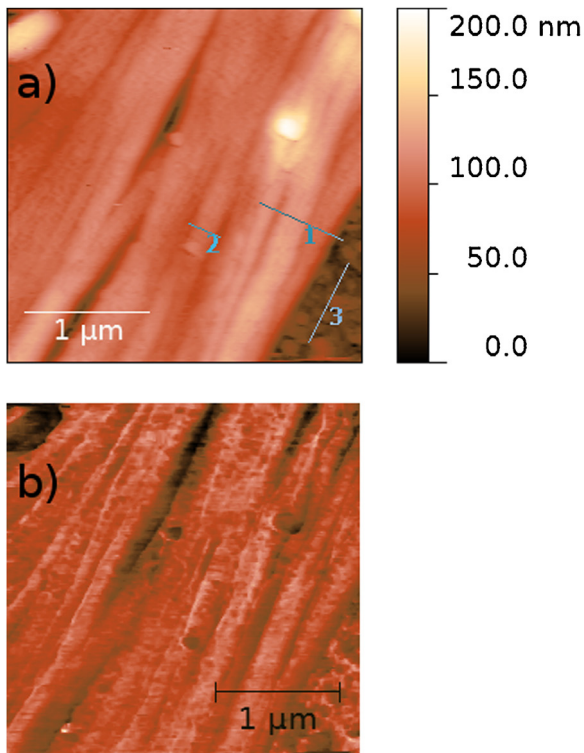


**Fig. 2.** AFM height (a) and friction (b) images of eumelanin deposit on a glass substrate. The images come from IE region of Fig. 1a. The line profiles in (c) refer to the three lines labeled in (a).

substrate (not shown in optical image of Fig. 1b) shown in Fig. 5. However, it is clearly evident in both height (Fig. 5a) and friction (Fig. 5b) images that such region is characterized by the presence of many point-like structures having height less than 10 nm and width less than 50 nm (line profile 2 in Fig. 5c), as well as grains with size similar to those in Fig. 4a (line profile 1 in Fig. 5c), whereas the contribution of mica substrate is almost negligible (line profile 3 in Fig. 5c). The point-like structures, which were not clearly evident on glass substrate probably because of the background ripple, suggest that the largest eumelanin granules might involve an internal structure based on the aggregation of such smaller point-like structures. The size of these small eumelanin structures results smaller than that found in (Jastrzebska et al., 2010) for similar synthetic eumelanin samples and it is comparable to the width and height of filamentous structures observed by Clancy and Simon (2001) in *S. officinalis* eumelanin deposited on mica substrate. Therefore, we can deduce from the similarity of morphological structures

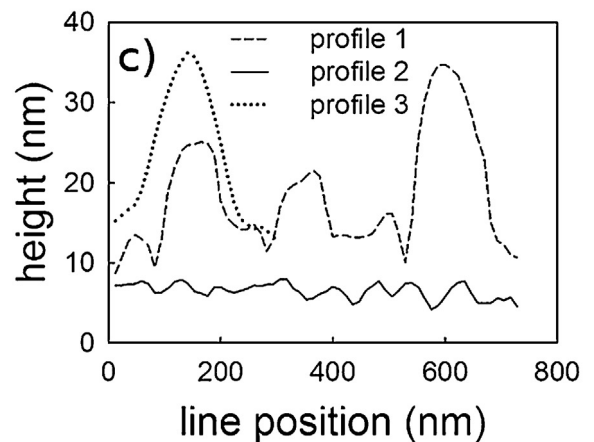
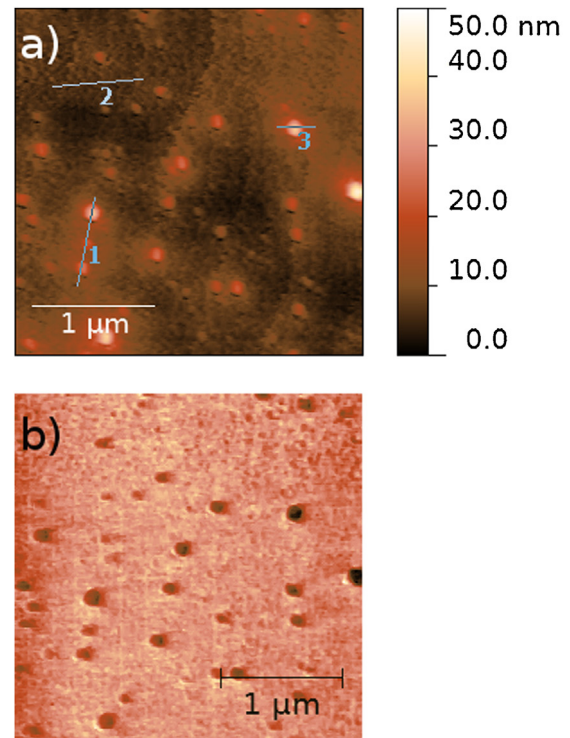


**Fig. 3.** AFM height (a) and friction (b) images of eumelanin deposit on a glass substrate. The images come from C region of Fig. 1a. The line profiles in (c) refer to the three lines labeled in (a).

observed in both synthetic and *S. officinalis* eumelanin that the model of synthetic eumelanin obtained from L-DOPA is suitable to investigate the structural properties of the natural pigment and that the role of proteins is almost negligible during the aggregation of the structural units to assemble the biopolymer.

As for the origin of filamentous structures, the lack of entanglement among them suggests they do not pre-exist in solution, but they are formed during the deposition and drying processes. The formation of a filament may occur by means of subsequent binding of eumelanin protomolecules through hydroxyl, carboxylic acid and amine groups. Attractive forces between the structural units and the substrate oppose to the aggregation of protomolecules and promote adsorption of eumelanin granules to the substrate. The larger negative charge of mica with respect to glass (Erikson et al., 1997) explains the larger density of isolated point-like eumelanin structures on mica substrate than on glass substrate.

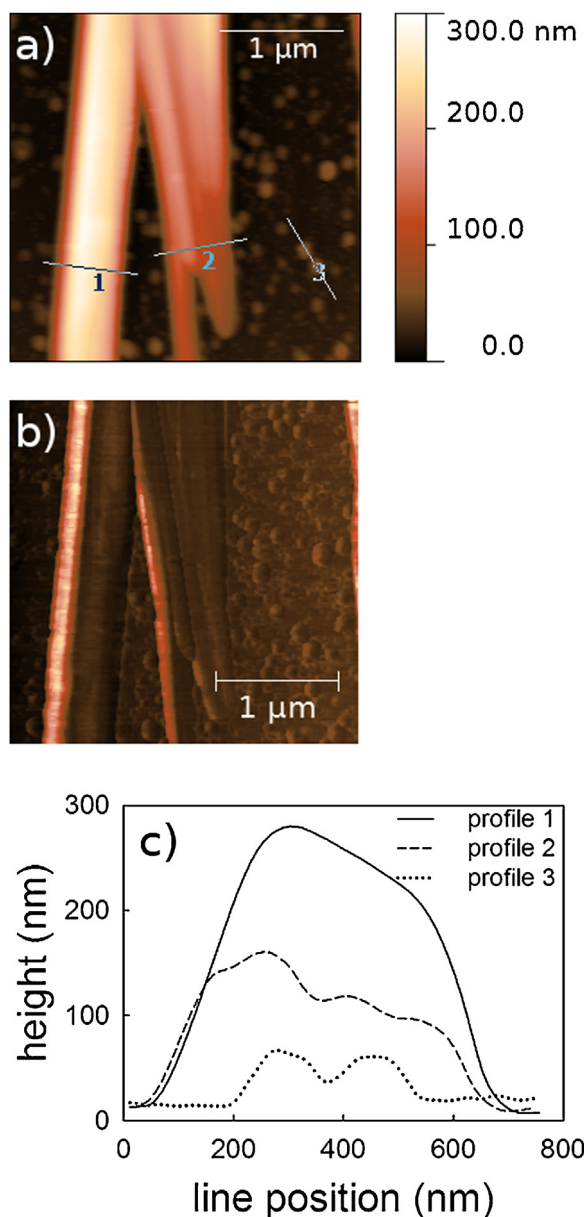


**Fig. 4.** AFM height (a) and friction (b) images of eumelanin deposit on a mica substrate. The images come from EE region of Fig. 1b. The line profiles in (c) refer to the three lines labeled in (a).

### 3.3. Dynamic light scattering

To confirm the presence of eumelanin nanoaggregates before the deposition process, the size distribution of eumelanin particles in aqueous solution has been investigated by means of DLS measurements, shown in Fig. 6. The size distribution of synthetic eumelanin particles has a main modal value centered at about 35 nm: such value is in agreement with the size of most eumelanin grains obtained by AFM measurements. The DLS returns, by Laplace transform inversion of the ACF, an intensity weighted size distribution. Accordingly, the distribution of Fig. 6 represents the fraction of light intensity scattered by particles of different size. This quantity depends either on the particle number either on particle size. The size dependence is dramatic, since the intensity of scattered light scales as the sixth power of the particle size. Therefore the intensity weighted size distribution is unavoidably biased toward larger

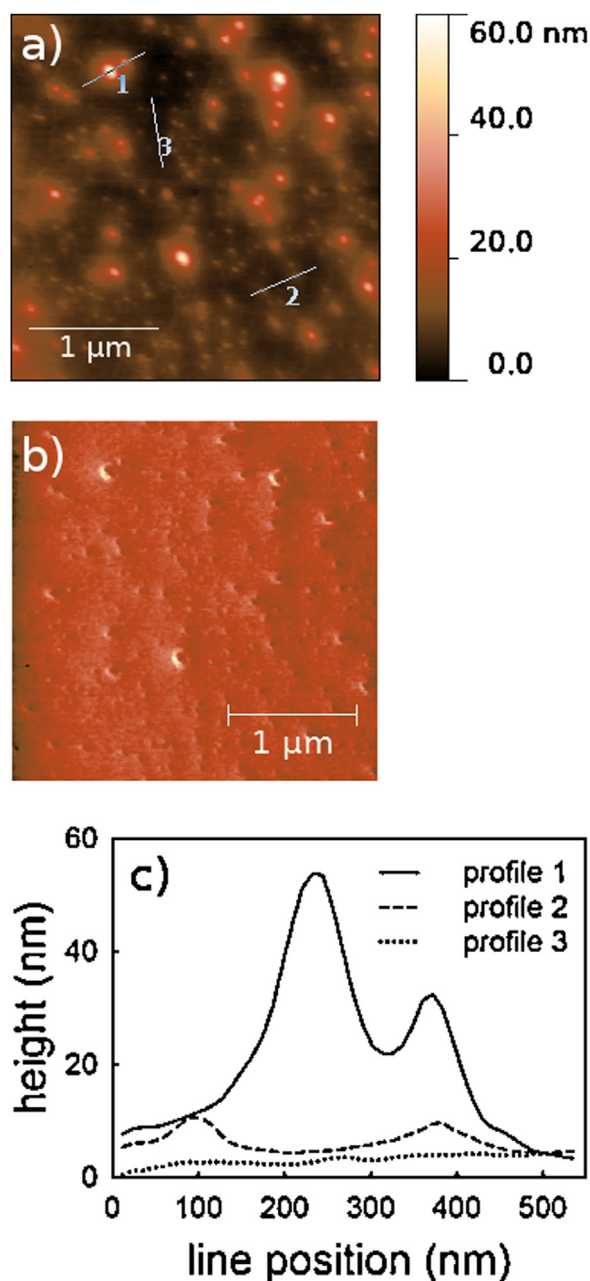


**Fig. 5.** AFM height (a) and friction (b) images of eumelanin deposit on a mica substrate. The images come from C region of Fig. 1b. The line profiles in (c) refer to the three lines labeled in (a).

particles. The presence of a large concentration of particles with sizes of tens of nanometers obscures any contribution of particles having size less than 10 nm that are visible in AFM images.

In addition, a weak bump centered at about 500 nm is also visible in Fig. 6, according to above discussion this is due to extremely rare aggregates. The partial aggregation in solution is promoted by interaction among eumelanin structural units and it is not hindered by the attractive interaction of eumelanin structures with the solid substrate. In addition, the above main modal value is also slightly smaller than that (about 70 nm) previously obtained by means of DLS measurements of synthetic eumelanin produced by oxidation of tyrosine with hydrogen peroxide (Perna et al., 2009). Therefore, DLS measurements emphasize that the dominant structures in eumelanin aqueous solution are particles with few tens nanometers size and, consequently, they aggregates themselves to

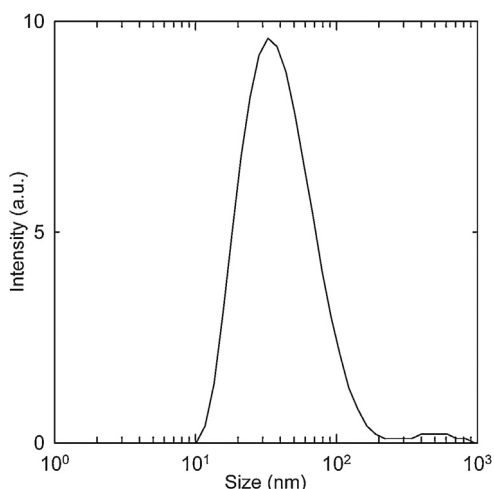


**Fig. 6.** Distribution of particles size for synthetic L-DOPA eumelanin solution, obtained by dynamic light scattering measurements at room temperature.

make granular and filamentous structures during the deposition and drying onto the different substrates.

#### 4. Conclusions

In conclusion, the presented AFM images show the presence of point-like eumelanin structures, few nanometer size, in synthetic eumelanin samples. The size of such structures is similar to that of previously imaged natural eumelanin aggregates (Clancy and Simon, 2001) and it results smaller than that reported for similar synthetic eumelanin samples (Jastrzebska et al., 2010). Such few nanometer size eumelanin structures are present in starting synthetic eumelanin solution, as revealed by DLS measurements. Furthermore, they aggregate themselves to make larger granular and filamentous aggregates after deposition on a solid substrate like glass or mica. As mica is more hydrophilic than glass, a larger number of eumelanin particles keep their point-like size after deposition on the former than on the latter substrate.

These results support the stacked oligomer model for eumelanin protomolecules and are interesting for the design and fabrication of electronic and photovoltaic materials based on eumelanin structure.

#### References

- Ambrico, M., Cardone, A., Ligonzo, T., Augelli, V., Ambrico, P.F., Cicco, S., Farinola, G.M., Filannino, M., Perna, G., Capozzi, V., 2010. Hysteresis-type current-voltage characteristics in Au/eumelanin/ITO/glass structure: towards melanin based memory devices. *Org. Electron.* 11, 1809–1814.
- Bridelli, M.G., 1998. Self-assembly of melanin studied by laser light scattering. *Biophys. Chem.* 73, 227–239.
- Clancy, C.M.R., Simon, J.D., 2001. Ultrastructural organization of eumelanin from *Sepia officinalis* measured by atomic force microscopy. *Biochemistry* 40, 13353–13360.
- Crippa, P.R., Horak, V., Prota, G., Svoronos, P., Wolfram, L., 1989. *The Alkaloids*. Academic Press Inc., New York.
- Erikson, C., Blomberg, E., Claesson, P., Nygren, H., 1997. Reactions of two hydrophilic surfaces with detergents, protein and whole human blood. *Colloids Surf. B* 9, 67–69.
- Gallas, J.M., Littrel, K.C., Seifert, S., Zajac, G.W., Thiagarajan, P., 1999. Solution structure of copper-ion induced molecular aggregates of tyrosine melanin. *Biophys. J.* 77, 1135–1142.
- Jastrzebska, M., Mroz, I., Barwinski, B., Wrzalik, R., Boryczka, S., 2010. AFM investigation of self-assembled DOPA-melanin nano-aggregates. *J. Mater. Sci.* 45, 5302–5308.
- Junker, P.J., Still, T., Lohr, M.A., Yodh, A.G., 2011. Suppression of the coffee-ring effect by shape-dependent capillary interactions. *Nature* 476, 308–311.
- Kruk, I., Lichszteid, K., Bounias, M., Kadna, A., Kubera-Nowakowska, L., 1999. Formation of active oxygen species during autoxidation of DOPA. *Chemosphere* 39, 443–453.
- Liu, Y., Simon, J.D., 2003. Isolation and biophysical studies of natural eumelanins: applications of imaging technologies and ultrafast spectroscopy. *Pigment Cell Res.* 16, 606–618.
- Mason, H.S., 1948. The chemistry of melanin: III. Mechanism of the oxidation of dihydroxyphenylalanine by tyrosinase. *J. Biol. Chem.* 172, 83–99.
- McQueenie, R., Sutter, J., Karolin, J., Birch, D.J.S., 2012. Eumelanin fibrils. *J. Biomed. Opt.* 17, 75001.
- Meredith, P., Powell, B.J., Riesz, J., Nighswander-Rempel, S.P., Pederson, M.R., Moore, E.G., 2006. Towards structure-property-function relationships for eumelanin. *Soft Matter* 2, 37–44.
- Meredith, P., Sarna, T., 2006. The physical and chemical properties of eumelanin. *Pigment Cell Res.* 19, 572–594.
- Morresi, L., Ficcadenti, M., Pinto, N., Murri, R., Cuccioloni, M., Angeletti, M., Tombesi, P., 2010. Optical and electrical behavior of synthetic melanin thin films spray-coated. *Energy Procedia* 2, 177–182.
- Nečas, D., Klapetek, P., 2012. Gwyddion: an open-source software for SPM data analysis. *Cent. Eur. J. Phys.* 10, 181–188.
- Perna, G., Frassanito, M.C., Palazzo, G., Gallone, A., Mallardi, A., Biagi, P.F., Capozzi, V., 2009. Fluorescence spectroscopy of synthetic melanin solution. *J. Lumin.* 129, 44–49.
- Perna, G., Palazzo, G., Mallardi, A., Capozzi, V., 2011. Fluorescence properties of natural eumelanin biopolymer. *J. Lumin.* 131, 1584–1588.
- Stark, K.B., Gallas, J.M., Zajac, G.W., Eisner, M., Golab, J.T., 2003. Spectroscopic study and simulation from recent structural models for eumelanin: II. Oligomers. *J. Phys. Chem. B* 107, 11558–11562.
- Watt, A.A.R., Bothma, J.P., Meredith, P., 2009. The supramolecular structure of melanin. *Soft Matter* 5, 3754–3760.
- Zeise, L., 1995. Analytical methods for characterization and identification of eumelanins. In: Zeise, L., Chedekel, M.R., Fitzpatrick, T.B. (Eds.), *Melanin: Its Role in Human Photoprotection*. Valdenmar Publishing, Overland Park, KS, pp. 65–79.